Cellular Automata Simulation of Arid Ecosystem Turing Patterns: A Cell-DEVS Reimplementation of the Hardenberg Model

Wenbin Wang
Systems and Computer Engineering
Carleton University
Ottawa, Canada
Student ID: 101191168
williamwang12@cmail.carleton.ca
Submitted to Prof. Gabriel A. Wainer

SYSC 5104 – Methodologies for Discrete Event Modelling and Simulation

***Abstract*—Vegetation in arid and semi-arid ecosystems often exhibits striking spatial patterns, such as spots, stripes, and labyrinths, which are classically explained by reaction-diffusion models based on Turing instability. In this project, we re-implement such vegetation pattern formation using a discrete-event cellular automata framework based on the Cell-DEVS formalism. Starting from well-known continuous models such as those by Hardenberg, Klausmeier, and Rietkerk, we reformulate soil moisture and biomass interactions into a modular, event-driven simulation environment. Our implementation, developed in C++ using the Cadmium DEVS engine, reproduces the emergence and evolution of self-organized vegetation structures while maintaining compatibility with discrete-event simulation techniques. This reimplementation provides a flexible and extensible platform for further experimentation, scaling, and visualization of dryland ecosystem dynamics.**

***Index Terms*—Turing patterns, arid ecosystems, vegetation modeling, reaction-diffusion systems, Cell-DEVS, Hardenberg model, DEVS**

Code Availability

The complete source code for this project is available at the following GitHub repository:
`gray-scott-cellular (GitHub)`

I. Introduction

Spatial patterns are widespread phenomena observed across various natural systems, from animal coat markings to ecological distributions and vegetation formations. Alan Turing first introduced a mathematical framework that explained how such complex patterns could spontaneously arise from the interplay between reaction and diffusion processes, known as the Turing mechanism [1]. These Turing patterns typically manifest as stripes, spots, or labyrinthine structures and have become a cornerstone of research in mathematical biology and ecology.

In this project, we first implemented a fundamental reaction-diffusion model using the Cell-DEVS formalism to simulate classical Turing patterns, utilizing the well-established Gray-Scott model [2]. This initial step validated the feasibility of using discrete-event simulation techniques to capture emergent spatial structures characteristic of Turing instability, demonstrating the capability of Cell-DEVS to model diffusion-driven self-organization with high modularity and flexibility.

Building upon this foundational work, we extended the simulation framework to model ecological phenomena, specifically focusing on vegetation pattern formation observed in semi-arid and arid regions. Our ecological modeling draws inspiration from seminal works by Klausmeier [3] and Rietkerk et al. [4], incorporating biologically meaningful variables such as soil moisture, plant biomass, and surface water. By reformulating these models within a discrete, event-driven framework, we enable fine-grained control over initial conditions, localized interactions, and heterogeneous diffusion processes, which are critical for studying realistic ecosystem dynamics.

Rather than proposing new ecological theories, this project emphasizes the reimplementation and demonstration of classical models within a modern simulation architecture. The resulting platform provides a flexible and extensible foundation for exploring vegetation pattern dynamics, facilitating further research into topics such as ecosystem resilience, spatial early-warning indicators, and the effects of environmental perturbations. Furthermore, the modular structure of Cell-DEVS makes it well-suited for future integration with GPU acceleration, remote sensing data, and machine learning techniques for large-scale ecological simulations.

Thus, our integrated modeling framework bridges theoretical foundations with practical ecological applications, offering both a validation tool for classical reaction-diffusion models and a scalable platform for future developments in ecological modeling and simulation.

II. Background

Pattern formation is a fascinating phenomenon seen across both natural and synthetic systems, where simple rules can

give rise to surprisingly complex structures. Alan Turing's groundbreaking work first explained how such patterns could emerge spontaneously through a mechanism now known as reaction-diffusion [1]. His theory showed that interactions between local reactions and diffusion processes can generate stable patterns such as spots, stripes, and labyrinths—patterns that are now recognized in fields ranging from biology to chemistry and ecology.

One of the best-known models capturing this idea is the Gray-Scott model, introduced by Gray and Scott in 1984 [2]. Thanks to its simple setup and rich dynamic behavior, the model became a popular framework for studying how localized reactions combined with diffusion can create diverse spatial patterns. Later, John E. Pearson [5] expanded on this work, showing that the Gray-Scott model could produce not just stationary spots, but also spirals, waves, and even chaotic patterns, highlighting its ability to represent complex spatial-temporal phenomena.

Since then, the Gray-Scott model has become a foundation for many biological modeling efforts. Researchers have used it to replicate patterning seen in animal skin pigmentation, coral growth, and even certain ecological systems like vegetation distributions [6].

Reaction-diffusion models have been especially valuable in ecological research. In semi-arid regions, vegetation often organizes itself into bands, spots, or maze-like patterns due to water scarcity and plant-water feedbacks. Klausmeier [3] proposed a simplified model explaining how these patterns form through the interaction between biomass growth and water movement. Building on this, Rietkerk et al. [4] emphasized how vegetation and water feedbacks drive self-organization, offering new ways to understand desertification and ecosystem stability.

More recently, Ge et al. [8] have demonstrated that Turing vegetation patterns in arid and semi-arid ecosystems exhibit long-range hyperuniformity—a spatial organization that enhances water-use efficiency and ecological resilience. Their findings connect theoretical reaction-diffusion modeling with real-world landscape management, suggesting that disruption of hyperuniform structures may critically reduce recovery capacity after disturbances.

Beyond ecology, reaction-diffusion theory has also shaped our understanding of developmental biology. It provides a powerful explanation for how organisms develop structures like limbs, organs, and pigmentation patterns from initially uniform cells [9], [10].

Overall, exploring Turing mechanisms through models like Gray-Scott and ecological vegetation frameworks not only deepens our understanding of how complex patterns arise, but also provides practical insights for studying real-world biological, ecological, and synthetic systems.

III. Turing Pattern

A. Model Definition and Simulation Framework

In this project, I implemented a complete simulation of the Gray-Scott reaction-diffusion model using the Cell-DEVS formalism to reproduce and analyze Turing patterns. This model, first popularized by John E. Pearson in 1993 [5], provides a mechanism by which two simple interacting chemicals—denoted as U and V—can give rise to rich, self-organizing spatial patterns through the combination of local reaction kinetics and diffusion.

The system is defined by the following irreversible reactions:

$$\mathrm{U} + 2\mathrm{V} \rightarrow 3\mathrm{V} \tag{1}$$

$$\mathrm{V} \rightarrow \mathrm{P} \tag{2}$$

where P is an inert product. A feed term F maintains a supply of U, while both U and V are subject to removal processes. These lead to the dimensionless partial differential equations that define the Gray-Scott system:

$$\frac{\partial U}{\partial t} = D_u \nabla^2 U - UV^2 + F(1-U) \tag{3}$$

$$\frac{\partial V}{\partial t} = D_v \nabla^2 V + UV^2 - (F+k)V \tag{4}$$

In these equations:

- D_u, D_v: Diffusion rates for chemicals U and V
- F: Feed rate for U
- k: Kill rate for V
- UV^2: Nonlinear reaction term responsible for pattern formation

To discretize the model for implementation in Cell-DEVS, I represent space as a 2D grid where each cell maintains a local state of u and v. Diffusion is approximated using a weighted 3×3 Laplacian kernel:

$$\begin{bmatrix} 0.05 & 0.2 & 0.05 \\ 0.2 & -1.0 & 0.2 \\ 0.05 & 0.2 & 0.05 \end{bmatrix}$$

This kernel allows each cell to receive contributions from its Moore neighborhood, thereby simulating diffusion.

Each cell evolves its state according to the reaction-diffusion dynamics:

$$\frac{du}{dt} = d_A \cdot \text{Laplacian}_u + f(1-u) - ruv^2 \tag{5}$$

$$\frac{dv}{dt} = d_B \cdot \text{Laplacian}_v - kv + ruv^2 \tag{6}$$

where r is the reaction rate (typically set to 1), and the concentrations are advanced using explicit Euler integration:

$$u' = u + \Delta t \cdot \frac{du}{dt} \tag{7}$$

$$v' = v + \Delta t \cdot \frac{dv}{dt} \tag{8}$$

An auxiliary variable v_{ratio} is calculated to help visualize the concentration balance between v and the total quantity $u+v$:

$$v_{\text{ratio}} = \begin{cases} \frac{v}{u+v} & \text{if } u+v > 0 \\ 0.5 & \text{otherwise} \end{cases} \tag{9}$$

B. Cell-DEVS Implementation

To simulate the model efficiently, I employed the Cadmium v2 simulation engine and structured the model using Cell-DEVS (Cellular Discrete Event System Specification). Cell-DEVS extends the classical DEVS formalism to handle spatially distributed systems.

Each cell in our simulation is defined as a Cell-DEVS atomic model:

- **State**: $S = \{(u, v) \in \mathbb{R}^2\}$
- **Inputs** X: From neighboring cells, concentrations (u, v)
- **Outputs** Y: Updated concentrations (u, v) to neighbors
- **Neighborhood**: Moore neighborhood (radius 1)
- **Transition Function** τ: Implements the Gray-Scott update using Laplacian + reaction terms
- **Time Advance** d: 1.0 (fixed timestep)

We implemented the Gray-Scott model in Cadmium v2 by instantiating a `GridCell<grayScottState>` for each lattice site and coupling them on a Moore radius-1 neighborhood. To formalize the behavior of each cell, we define the atomic model `GrayScottCell` using the standard Cell-DEVS nine-tuple notation.

1) GrayScottCell: Atomic Cell-DEVS Model: Each lattice site is realized as a Cell-DEVS atomic model, `GrayScottCell`, defined by the nine-tuple

$$\text{GrayScottCell} = \big\langle X,\ Y,\ S,\ N,\ \tau,\ \delta_{\text{int}},\ \delta_{\text{ext}},\ \lambda,\ d \big\rangle.$$

- X External inputs: $\{\,(u, v) \in \mathbb{R}^2\}$. Each neighbor sends its current concentrations (u, v).
- Y External outputs: $\{\,(u, v) \in \mathbb{R}^2\}$. After updating, the cell emits its new (u, v) to all neighbors.
- S Internal state: $\{(u, v) \mid u, v \in \mathbb{R}\}$, initialized to $(1.0, 0.0)$. A derived ratio $v_{\text{ratio}} = v/(u + v)$ is also stored for visualization.
- N Neighborhood: Moore radius-1, i.e. $\{(i + \Delta r, j + \Delta c) \mid \Delta r, \Delta c \in \{-1, 0, 1\}\}$.
- τ Local transition (computed every internal step): nosep,leftmargin=*
  1) Compute discrete Laplacian using the weight kernel $\begin{bmatrix} 0.05 & 0.2 & 0.05 \\ 0.2 & -1.0 & 0.2 \\ 0.05 & 0.2 & 0.05 \end{bmatrix}$.
  2) Evaluate reaction–diffusion rates
  $$\frac{du}{dt} = d_A \nabla^2 u + f(1 - u) - r\, u\, v^2,$$
  $$\frac{dv}{dt} = d_B \nabla^2 v - k\, v + r\, u\, v^2.$$
  3) Advance concentrations by explicit Euler:
  $$u \leftarrow u + \Delta t\, \frac{du}{dt}, v \leftarrow v + \Delta t\, \frac{dv}{dt}.$$

  Typical parameters used in the simulation are $f = 0.5$, $k = 0.32$, $r = 1.0$, $d_A = 0.2$, $d_B = 0.1$, $\Delta t = 1.0$. These values are based on those provided in the Biological Modeling Project [6].
- δ_{int} Internal transition: Fires every d time units to invoke τ and update (u, v).
- δ_{ext} External transition: Buffers early arrivals of (u, v) inputs until the next internal event.
- λ Output function: Immediately after each internal transition, emits the current state (u, v).
- d Time advance: Constant $d = 1.0$, so each cell updates at uniform intervals of one time unit.

2) Coupled Gray-Scott Grid: Network DEVS Model: The entire $m \times n$ grid is coupled into a network model

$$\text{Grid}_{\text{GS}} = \big\langle \mathit{Xlist},\ \mathit{Ylist},\ I,\ X,\ Y,\ \eta,\ N,\ (m, n),\ C,\ B,\ Z,\ \text{select} \big\rangle,$$

where:

- $\mathit{Xlist} = \mathit{Ylist} = \varnothing$ (no external I/O ports).
- I is a trivial interface since $\mathit{Xlist} = \mathit{Ylist} = \varnothing$.
- $X = Y = \mathbb{R}^2$ (message type is the (u, v) pair).
- (m, n): grid dimensions (e.g. $m = n = 101$).
- $\eta = m \times n$: total number of cells.
- N: Moore radius-1 neighbor offsets as above.
- $C = \{C_{ij} \mid 0 \le i < m,\ 0 \le j < n\}$, each $C_{ij} = \langle X, Y, S, N, \tau, \delta_{\text{int}}, \delta_{\text{ext}}, \lambda, d \rangle$ is a `GrayScottCell`.
- $B = \varnothing$: no internal couplings beyond neighborhood links.
- Z: coupling map—each cell's output port to the matching neighbor's input port with periodic (wrap-around) indexing.
- select: default tie-breaking (e.g. row-major order) for simultaneous events.

This specification directly corresponds to the Cadmium v2 implementation, where each `GridCell<grayScottState>` handles buffering, timing, and neighbor messaging according to the Cell-DEVS rules outlined above.

IV. Turing Vegatation Pattern

To extend the classical Gray-Scott reaction-diffusion framework into ecological systems, I implemented the Hardenberg model [7] for vegetation pattern formation in arid landscapes. This model captures the interaction between two key variables over time and space: plant biomass density and soil moisture . It builds upon the idea that differential diffusion and nonlinear feedback between vegetation and water availability can produce stable, self-organized spatial structures such as vegetation bands, spots, and gaps, often referred to as Turing vegetation patterns.

A. Model Definition and Simulation Framework

The mathematical formulation of the Hardenberg model, based on the equations proposed in the literature [4], is as follows:

$$\frac{\partial B}{\partial t} = \frac{\gamma S}{1 + \sigma S} B - B^2 - \mu B + D_B \nabla^2 B \tag{10}$$

$$\frac{\partial S}{\partial t} = p - (1 - \phi B) S - S^2 B + \delta \nabla^2 (S - \beta B) \tag{11}$$

where:

- B: biomass density (vegetation coverage),
- S: soil moisture (available water),
- γ: maximum specific growth rate of vegetation,
- σ: saturation constant (controls response to soil moisture),
- μ: mortality rate of biomass,
- D_B: diffusion coefficient for vegetation spread,
- p: rainfall or external water input,
- ϕ: vegetation infiltration enhancement factor,
- β: water uptake per unit biomass,
- δ: diffusion coefficient for soil water.

These equations include:

1) A vegetation growth term that increases with available soil moisture but saturates at high levels.
2) Biomass loss via competition and natural decay .
3) Soil moisture dynamics including input from precipitation , loss from evaporation , and plant uptake .
4) Differential diffusion of water and biomass, including a cross-diffusion term that captures reduced infiltration in vegetated regions.

B. Cell-DEVS Implementation

I implemented this model using the Cadmium v2 Cell-DEVS simulation engine, which allows spatiotemporal systems to be represented as grids of interconnected cells. Each cell in the model maintains its own state variables and , which are updated according to reaction-diffusion equations.

The key components of the implementation include:

- **States**: Each cell contains its own soil moisture and biomass values, .
- **Neighborhood**: A von Neumann neighborhood (top, bottom, left, right) is used to approximate spatial diffusion.
- **Laplacian Approximation**: For each cell, the discrete Laplacian is computed as:

$$\nabla^2 B \approx \frac{1}{dx^2}\left(\sum_{\text{neighbors}} B_{ij} - NB\right) \tag{12}$$

$$\nabla^2(S-\beta B) \approx \frac{1}{dx^2}\left(\sum_{\text{neighbors}} (S_{ij}-\beta B_{ij}) - N(S-\beta B)\right) \tag{13}$$

  where for a von Neumann neighborhood, and .
- **Time Integration**: Using Euler integration with a small timestep , the update rules are:

$$B' = B + \Delta t\left(\frac{\gamma S}{1+\sigma S}B - B^2 - \mu B + \nabla^2 B\right) \tag{14}$$

$$S' = S + \Delta t\left(p - (1-\phi B)S - S^2 B + \delta\nabla^2(S-\beta B)\right) \tag{15}$$

- **Stability Handling**: To prevent non-physical values, I enforce , after each update.

This setup enables the emergence of classical Turing vegetation patterns. By varying the precipitation parameter and other coefficients, I observed a range of steady-state and oscillatory behaviors: vegetation bands, spot replication, front propagation, and eventual collapse at low rainfall. The simulation's periodic boundaries ensure seamless pattern propagation.

1) VegetationCell: Atomic Cell-DEVS Model: Each patch is implemented as a Cell-DEVS atomic model, `VegetationCell`, defined by

$$\text{VegetationCell} = \big\langle X,\ Y,\ S,\ N,\ \tau,\ \delta_{\text{int}},\ \delta_{\text{ext}},\ \lambda,\ d\big\rangle.$$

X External inputs: $\{(S,B) \in \mathbb{R}^2\}$. Each neighbor sends its soil moisture S and biomass B.

Y External outputs: $\{(S,B) \in \mathbb{R}^2\}$. After updating, the cell emits its new (S,B) to all neighbors.

S Internal state: $\{(S,B) \mid S,B \in \mathbb{R}\}$, initialized to $(1.0, 0.0)$.

N Neighborhood: von Neumann radius–1, $\{(i+\Delta r, j+\Delta c) \mid \Delta r, \Delta c \in \{-1,0,1\}, |\Delta r| + |\Delta c| \le 1\}$.

τ Local transition (executed every internal step):

1) Compute cross-diffusion terms:

$$sb_0 = S - \beta B, \quad \nabla^2(sb) = \tfrac{1}{\Delta x^2}\Big(\sum sb_{\text{nb}} - 4\, sb_0\Big),$$

$$\nabla^2 B = \frac{1}{\Delta x^2}\Big(\sum B_{\text{nb}} - 4\,B\Big).$$

2) Evaluate rates:

$$\dot S = p - (1-\phi B)\,S - S^2 B + \delta\,\nabla^2(sb),$$

$$\dot B = \frac{\gamma S}{1+\sigma S}\,B - B^2 - \mu B + \nabla^2 B.$$

3) Euler update: $S \leftarrow S + \dot S\,\Delta t, \quad B \leftarrow B + \dot B\,\Delta t.$

The typical initial parameters used in the Hardenberg model are: $\gamma = 1.6$, $\sigma = 1.6$, $\mu = 0.2$, $\phi = 1.5$, $\beta = 3.0$, $\delta = 100.0$, $p = 0.15$, $\Delta t = 5 \times 10^{-4}$, $\Delta x = 0.5$.

δ_{int} Internal transition: Fires every d time units to invoke τ.

δ_{ext} External transition: Buffers early arrivals of (S,B) until the next internal event.

λ Output function: After each internal transition, emits the updated (S,B).

d Time advance: Constant $d = 1.0$ time unit.

2) Coupled Vegetation Grid: Network DEVS Model: The full $m \times n$ landscape is assembled into

$$\text{Grid}_{\text{Veg}} = \big\langle Xlist,\ Ylist,\ I,\ X,\ Y,\ \eta,\ N,\ (m,n),\ C,\ B,\ Z,\ \text{select}\big\rangle,$$

where:

- $Xlist = Ylist = \varnothing$ (no external ports).
- $X = Y = \mathbb{R}^2$ (messages carry (S,B) pairs).
- (m,n) are grid dimensions (e.g. 101×101).
- $\eta = m\,n$ is total cells.
- N is the von Neumann neighbor set above.
- $C = \{C_{ij}\}$, each C_{ij} = VegetationCell.
- $B = \varnothing$ (no extra couplings).
- Z maps each cell's output port to its four neighbors' input ports with wrap-around.
- select is the default row-major tie-break.

V. Simulation results

This section presents the outcomes of the numerical experiments for both the Gray-Scott reaction–diffusion model and the Hardenberg vegetation model. For the Gray-Scott system, I demonstrate how varying feed rate and kill rate produces classical Turing patterns including spots, stripes, and labyrinths. Spatial snapshots at representative time steps illustrate the onset and stabilization of these patterns. For the vegetation model, I show the emergence of banded vegetation and spotty patches as precipitation and biomass growth parameters change.

A. Turing Pattern

1) Simulation Setup 1: In order to observe the formation of Turing patterns, I initialized the Gray-Scott model on a 101×101 grid with periodic boundary conditions. The initial concentrations of U and V were set to 1.0 and 0.0 respectively, with small perturbations seeded randomly across the grid. The following parameter values were used throughout the experiments:

- Feed rate (f): 0.055
- Kill rate (k): 0.117
- Reaction rate constant (r): 1.0
- Diffusion coefficient of chemical u (d_A): 1.0
- Diffusion coefficient of chemical v (d_B): 0.5
- Time step (Δt): 1.0
- Placed one 4 x 4 spots in the centre of the grid

As shown in Fig. 1, the pattern undergoes a continuous transformation. Initially, the perturbation expands radially to form a circular ring (Steps 500–2000). The ring gradually thickens and stabilizes into a square-shaped boundary due to symmetry breaking (Steps 2500–3500). In the later stages, the structure begins to exhibit inward bending and branching, eventually developing into a complex, cross-like symmetric pattern by Step 10,000.

2) Simulation Setup 2: To further explore the influence of reaction and diffusion parameters on pattern formation, a second experiment was conducted with modified settings. The Gray-Scott model was again initialized on a 101×101 grid with periodic boundary conditions, and random perturbations were introduced to the initial concentrations of U and V.

The following parameter values were used in this simulation:

- Feed rate (f): 0.042
- Kill rate (k): 0.101
- Reaction rate constant (r): 1.0
- Diffusion coefficient of chemical u (d_A): 0.195
- Diffusion coefficient of chemical v (d_B): 0.1
- Time step (Δt): 1.0
- Randomly placed 20 spots, each of size 3×3, across the grid.

As shown in Fig. 1, the Gray-Scott model evolves from sparse, randomly initialized perturbations into complex spatial patterns. In the early stages (Step 0 to Step 300), small isolated spots begin to grow and form ring-like structures due to local reaction-diffusion dynamics. Between Step 450 and Step 900, these rings interact and deform as they begin to coalesce, giving rise to square-like boundaries and emerging connections. From Step 1050 onward, the system transitions into a dense labyrinth-like pattern composed of interconnected stripes and loops. By Step 2000, the pattern stabilizes into a quasi-stationary structure characteristic of the Gray-Scott regime.

This hybrid morphology represents a transitional phase between the classic spot-dominated and stripe-dominated regimes. The selected parameter combination—particularly the moderate feed rate and the diffusion imbalance ($d_A/d_B \approx 1.95$)—promotes short-range activation and long-range inhibition, supporting the coexistence of both motifs. The resulting configuration (Fig. 2) is consistent with previously reported Gray-Scott phase spaces [5].

3) Simulation Setup 3: To further explore the effect of reaction and diffusion parameters on pattern formation, a third experiment was carried out with modified settings, while keeping the initial conditions identical to the previous setup.

The following parameter values were used in this simulation:

- Feed rate (f): 0.042
- Kill rate (k): 0.0907
- Reaction rate constant (r): 1.0
- Diffusion coefficient of chemical u (d_A): 0.195
- Diffusion coefficient of chemical v (d_B): 0.1
- Time step (Δt): 1.0
- Randomly placed 20 spots, each of size 3×3, across the grid.

Fig. 3 shows the evolution of spatial patterns in the Gray-Scott reaction-diffusion model under Setup 2. Random perturbations in the initial concentrations of species U and V quickly lead to localized circular activations. As the simulation progresses (Steps 150–900), these grow into ring-like or square structures through nonlinear reaction-diffusion dynamics. From Steps 1050 to 1650, the system transitions into a dense, tiled configuration of nested square and cross-shaped motifs. By Step 2500, it stabilizes into a symmetric, quasi-stationary pattern, highlighting the model's ability to generate complex structures from simple local rules.

4) Discussion: The final steady-state patterns are highly sensitive to the system parameters, particularly the feed rate (f), kill rate (k), and the diffusion coefficient ratio D_u/D_v. As predicted by theoretical analyses, increasing the feed rate generally destabilizes isolated spot formations, giving rise to stripe-like or labyrinthine patterns. Conversely, lowering the feed rate favors the persistence of localized spots.

These findings are consistent with the classification of pattern regimes presented by Pearson [5], and align well with the behavior described in the Gray-Scott model overview [6]. The observed transitions between spot and stripe phases illustrate the model's capacity to reproduce a diverse range of biologically inspired Turing patterns under simple initial conditions.

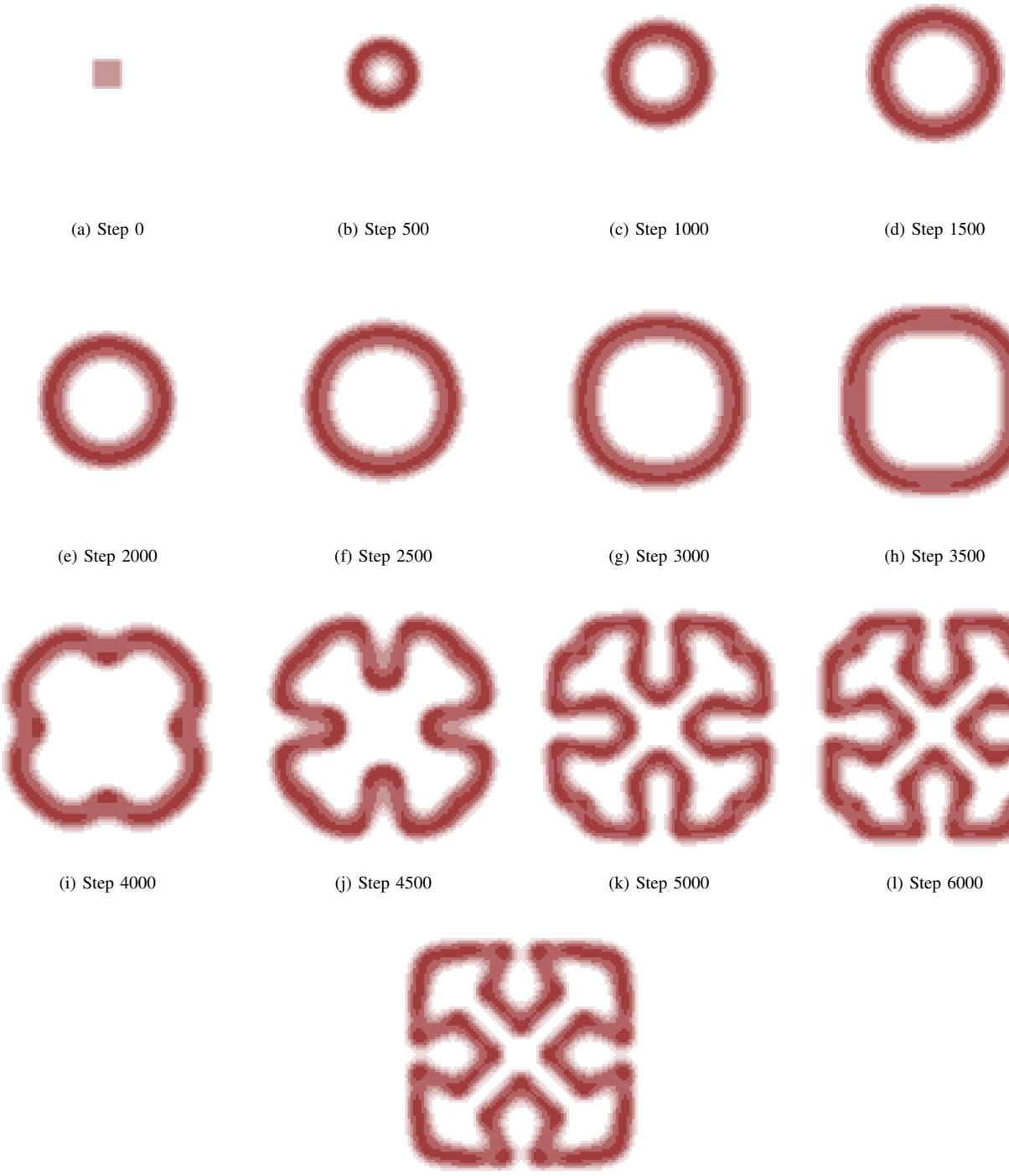

(a) Step 0 (b) Step 500 (c) Step 1000 (d) Step 1500

(e) Step 2000 (f) Step 2500 (g) Step 3000 (h) Step 3500

(i) Step 4000 (j) Step 4500 (k) Step 5000 (l) Step 6000

(m) Step 10000

Fig. 1: Pattern evolution over time steps in the simulation. A single perturbation gradually transforms into complex, symmetric patterns due to reaction-diffusion dynamics.

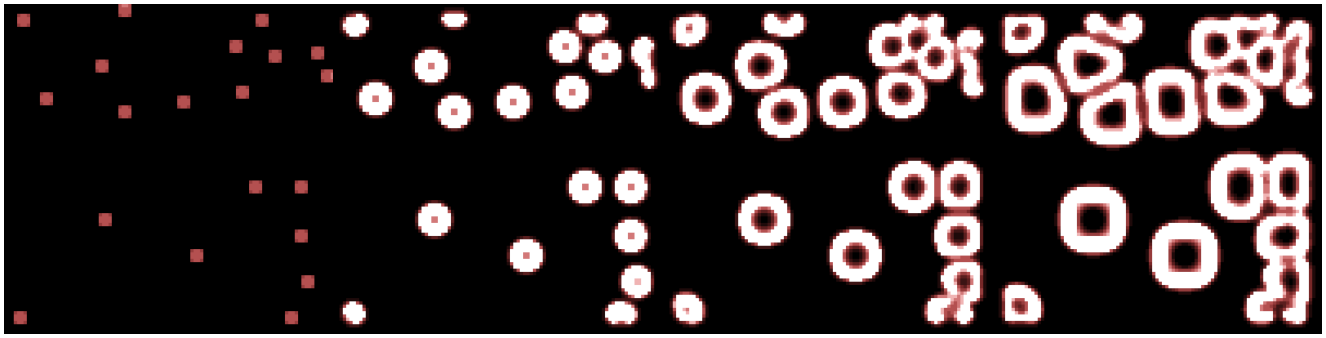

(a) Step 0 (b) Step 150 (c) Step 300 (d) Step 450

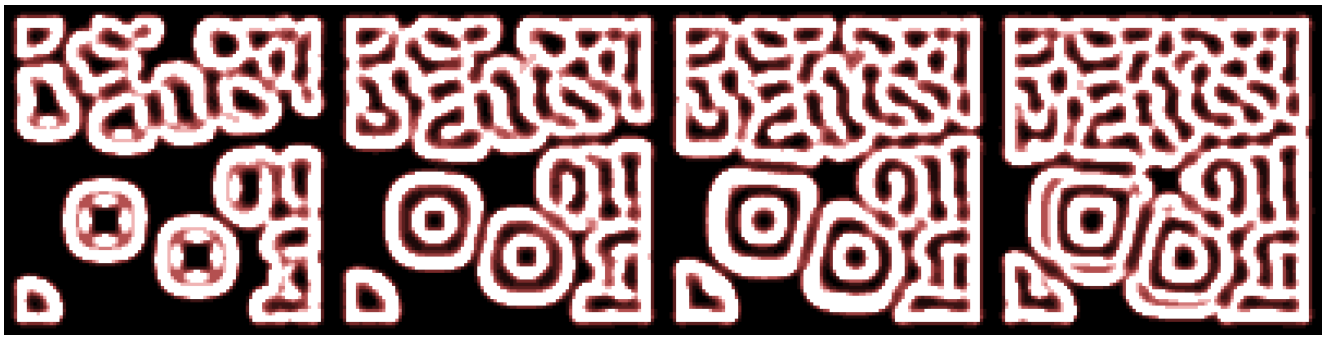

(e) Step 600 (f) Step 750 (g) Step 900 (h) Step 1050

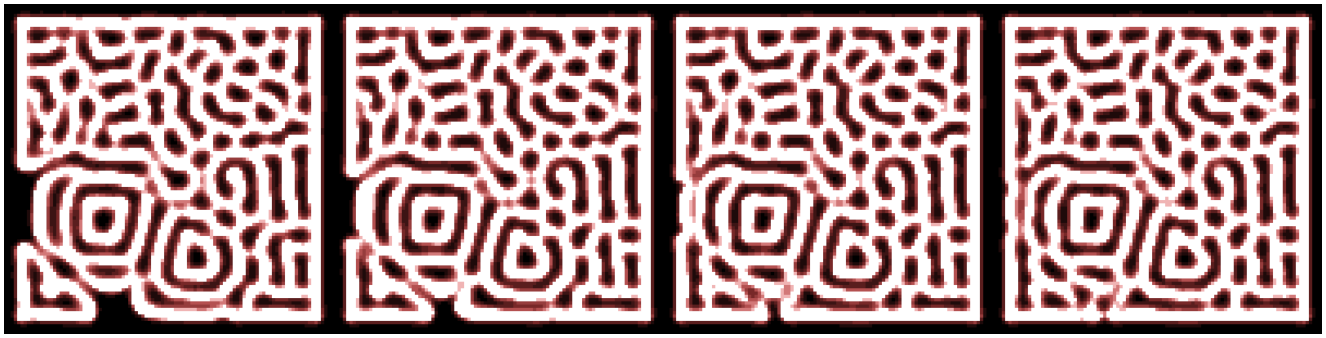

(i) Step 1200 (j) Step 1350 (k) Step 1500 (l) Step 1650

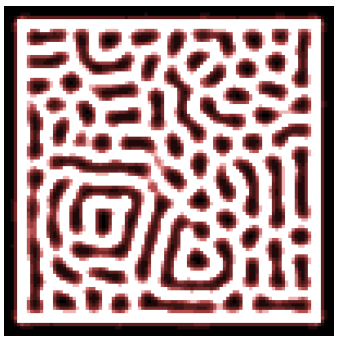

(m) Step 2000

Fig. 2: Evolution of spot-stripe hybrid pattern under Simulation Setup 2. A random initial perturbation evolves into a stable configuration with both isolated spots and stripe-like segments.

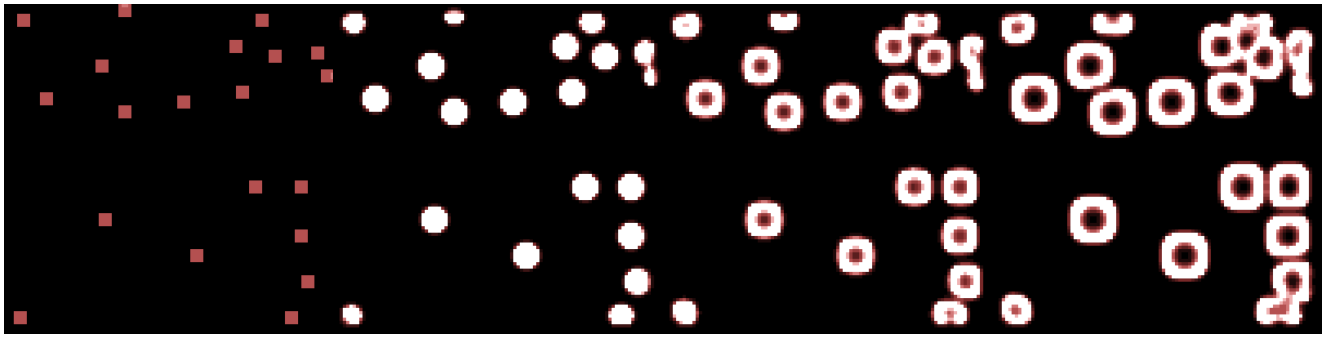

(a) Step 0 (b) Step 150 (c) Step 300 (d) Step 450

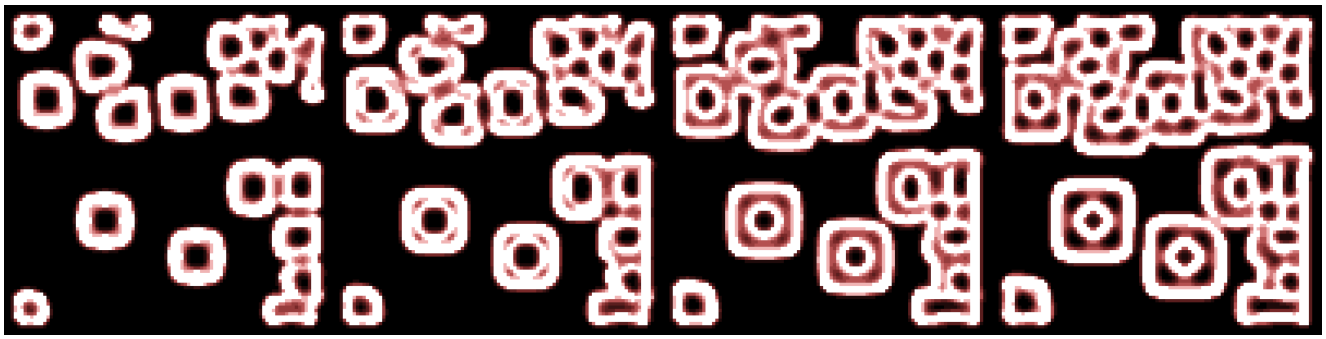

(e) Step 600 (f) Step 750 (g) Step 900 (h) Step 1050

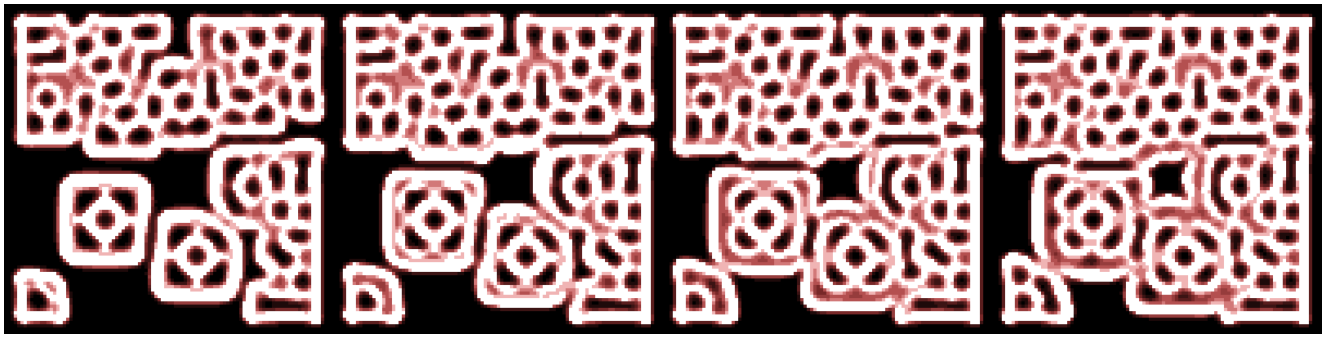

(i) Step 1200 (j) Step 1350 (k) Step 1500 (l) Step 1650

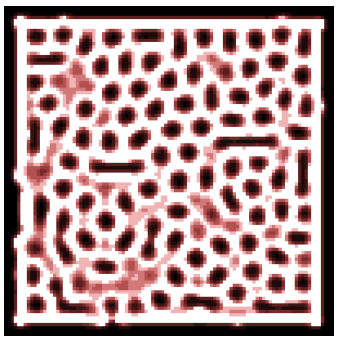

(m) Step 2500

Fig. 3: Evolution of dot-like patterns over time steps in the simulation, showing the transformation from initial perturbations to complex, symmetric structures due to reaction-diffusion dynamics.

B. Turing Vegatation Pattern

1) Simulation Setup 1: To explore the effects of both high initial biomass coverage and low precipitation on vegetation pattern formation, we conducted Simulation Setup 1 using a 10% initial perturbation—where 10% of the grid cells were randomly initialized with $B = 2.0$, representing active biomass. The simulation was run on a 101×101 periodic grid using the following parameters:

- Feed rate (p): 0.05
- Growth rate constant (γ): 1.6
- Moisture sensitivity (σ): 1.6
- Mortality rate (μ): 0.2
- Water uptake coefficient (ϕ): 1.5
- Diffusion rate of water (δ): 100.0
- Coupling factor (β): 3.0
- Time step (Δt): 0.0005
- Spatial discretization (Δx^2): 0.25

As shown in Figure 4, the initially sparse vegetation rapidly expands due to the high precipitation rate ($p = 4.0$), resulting in broad patches of biomass across the grid. Compared to Setup 1 with lower rainfall, the increased water availability enables more sustained growth, allowing local clusters to merge and form larger, interconnected regions.

Despite this expansion, the relatively low initial biomass density prevents the system from reaching complete coverage. Instead, the vegetation organizes into irregular but stable patches, with visible gaps and boundaries—resembling spot-like or fragmented Turing structures. This behavior highlights how both precipitation and initial seeding density jointly influence the emergent spatial organization.

2) Simulation Setup 2: In this experiment, we investigate the influence of high precipitation on vegetation pattern formation under sparse initial conditions. Simulation Setup 2 initializes only 2.5% of the grid cells with $B = 2.0$ (active biomass), simulating a scenario where vegetation is initially scarce. The system is run on a 101×101 periodic grid with the following parameter settings:

- Precipitation rate (p): 4.0
- Growth rate constant (γ): 1.6
- Moisture sensitivity (σ): 1.6
- Mortality rate (μ): 0.2
- Water uptake coefficient (ϕ): 1.5
- Diffusion rate of water (δ): 100.0
- Coupling factor (β): 3.0
- Time step (Δt): 0.0005
- Spatial discretization (Δx^2): 0.25

As shown in Figure 5, the initially sparse vegetation gradually expands and self-organizes into a dispersed spot-like pattern. Despite the high precipitation rate ($p = 4.0$), the low initial biomass density limits the extent of spatial spread and prevents neighboring clusters from merging. As a result, vegetation remains fragmented into isolated patches rather than forming continuous or striped coverage.

This outcome aligns with classical reaction-diffusion theory in arid and semi-arid systems, where positive feedback between vegetation growth and moisture uptake leads to stable localized structures. The simulation highlights that even under favorable rainfall conditions, the initial biomass seeding strongly influences the system's trajectory—determining whether the final pattern manifests as spotted, striped, or uniform.

3) Discussion: This work demonstrates how discrete-event modeling, implemented via the Cell-DEVS formalism, can effectively reproduce self-organizing vegetation patterns predicted by continuous reaction-diffusion theory. By simulating vegetation dynamics with local water-plant feedback and nonlinear diffusion, our model reproduces a rich diversity of spatiotemporal structures, including spotted, striped, and transitional regimes, depending on initial biomass density and precipitation rate (p). These findings are consistent with the pioneering work of Hardenberg et al. [4], where a continuous partial differential equation (PDE) model revealed that vegetation patterns can emerge purely from ecological interactions mediated by water transport.

Compared to the continuous PDE-based simulations in Hardenberg's model, our DEVS-based framework offers a discrete, asynchronous, and event-driven alternative that maintains spatial and temporal resolution flexibility. Unlike traditional finite-difference integration, the Cell-DEVS model benefits from localized updates and is easily extensible to complex boundary conditions, heterogeneous terrain, or multiple interacting species. Moreover, our Cell-DEVS simulations qualitatively reproduce key behaviors described in [4]: at low precipitation ($p \approx 0.05$), sparse biomass leads to isolated spots; at intermediate p, stripe-like labyrinths may form; and at high p, vegetation expands but stabilizes in spotted or homogeneous states, depending on initial conditions.

Importantly, our results also highlight the influence of initial biomass seeding. In contrast to most PDE studies that assume infinitesimal noise or homogeneous initial states, we explicitly control the perturbation density (e.g., 2.5%, 10%) and find that pattern formation is highly sensitive to these initial conditions—consistent with the hysteresis and multistability discussed in both [4] and [8]. This suggests that discrete modeling may be particularly useful in exploring questions of ecosystem resilience, tipping points, and recovery potential after degradation or intervention.

In summary, our DEVS-based approach complements continuous models by offering fine-grained control over initial conditions, local rules, and discrete update mechanisms. It supports scalable, modular simulation of ecological self-organization and provides a promising platform for integrating field data, exploring non-equilibrium transitions, and informing desertification risk assessments.

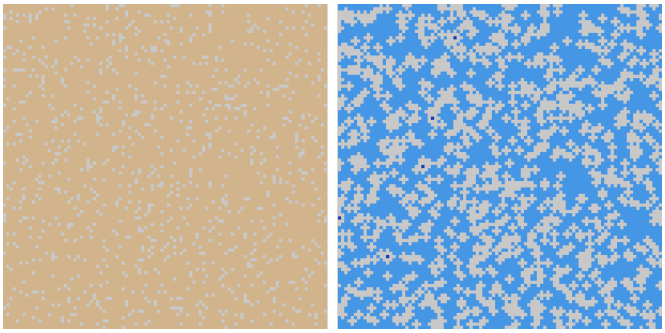

(a) Step 0

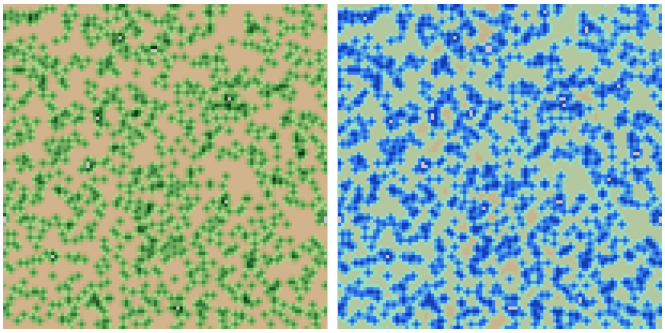

(b) Step 200

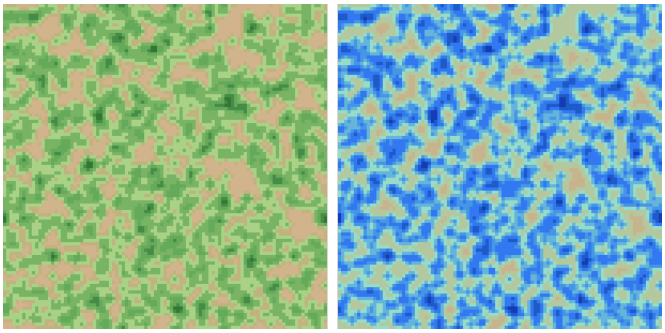

(c) Step 400

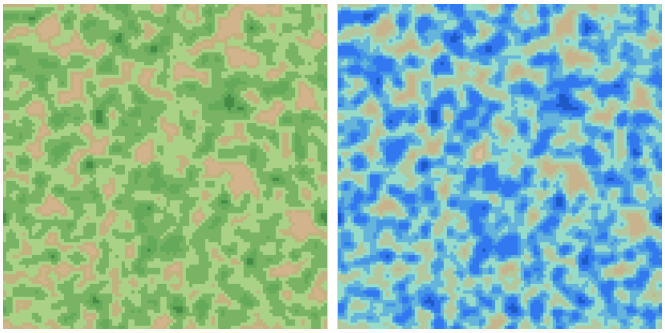

(d) Step 600

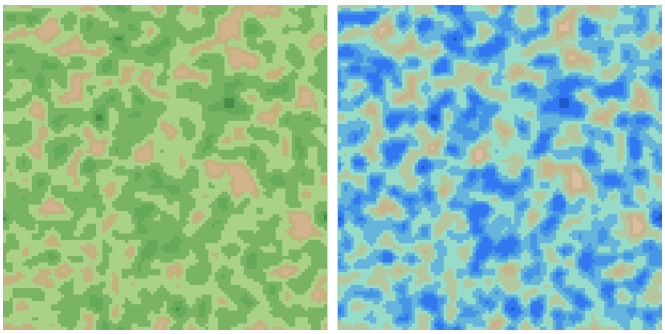

(e) Step 800

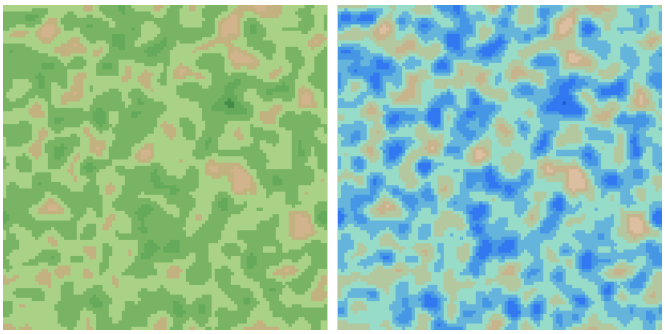

(f) Step 1000

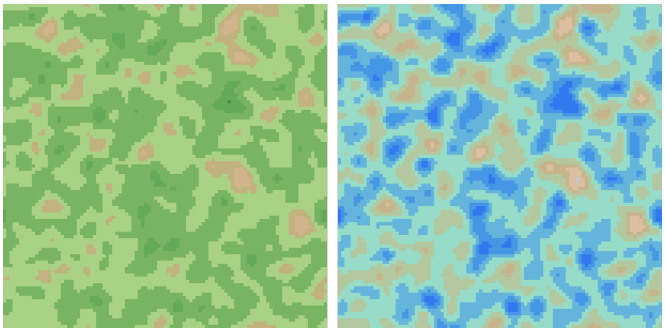

(g) Step 1200

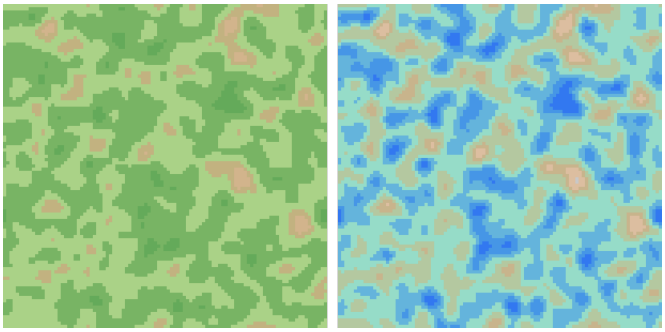

(h) Step 1225

Fig. 4: Evolution of patterns in Simulation Setup 1 with 10% of the cells are initialized with $B = 2$ (active biomass). Selected frames demonstrate how the system evolves from randomly scattered initial seeds into complex spatial organizations driven by reaction-diffusion dynamics.

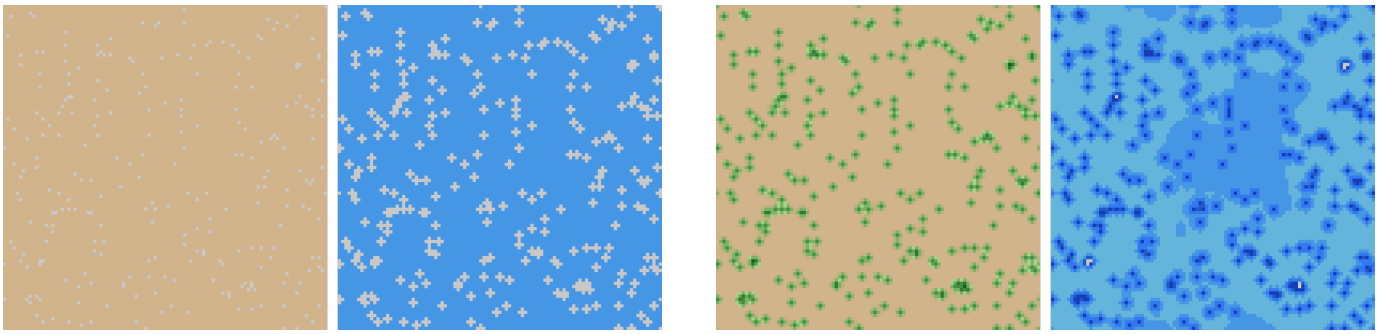

(a) Step 0

(b) Step 200

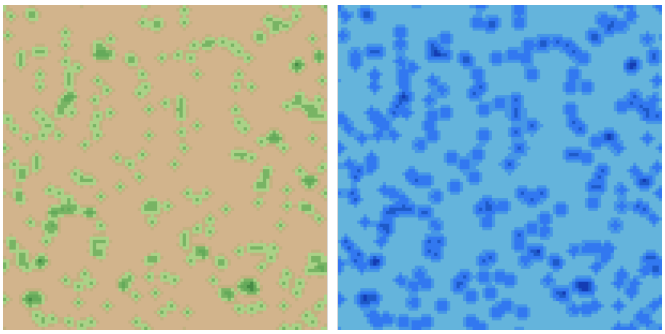

(c) Step 400

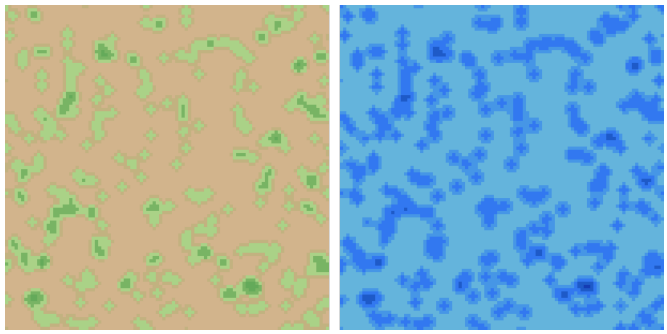

(d) Step 600

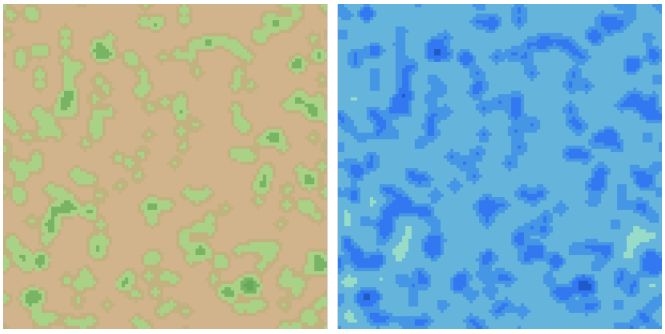

(e) Step 800

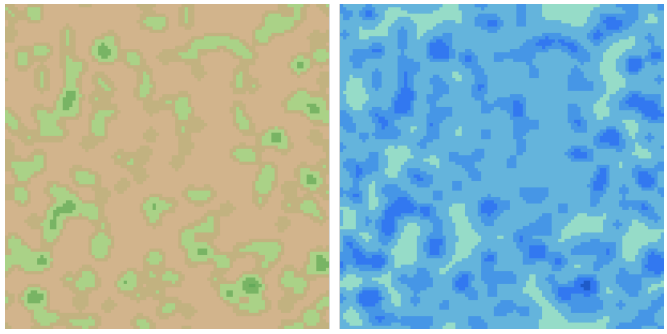

(f) Step 1000

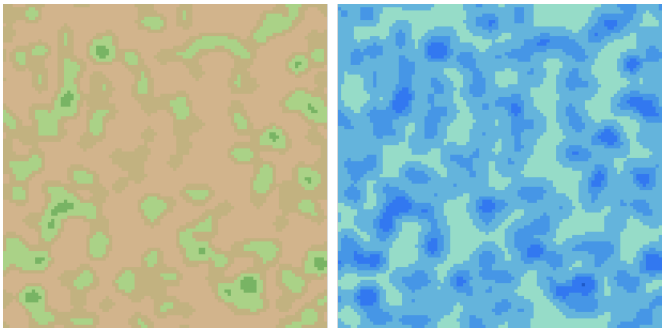

(g) Step 1200

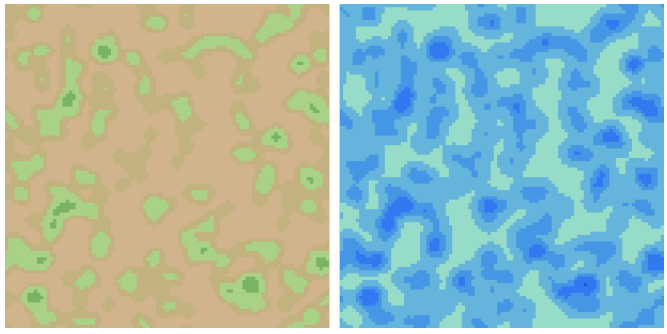

(h) Step 1225

Fig. 5: Evolution of vegetation and soil moisture patterns in Simulation Setup 2 with 2.5% of the cells are initialized with $B = 2$ (active biomass). As the system evolves, small localized biomass clusters grow and stabilize into a spotted pattern characteristic of arid environments under low precipitation conditions. The left panel of each subfigure shows biomass B, and the right panel shows soil moisture S.

VI. Conclusions

In this project, we successfully implemented and validated a discrete-event simulation framework for reaction-diffusion systems and vegetation pattern formation, leveraging the Cell-DEVS formalism. Our models reproduced classic Turing patterns, including spots, stripes, and labyrinths in the Gray-Scott system, as well as vegetation patchiness under the Hardenberg model for arid ecosystems. The discrete, modular structure of Cell-DEVS enabled flexible experimentation with local dynamics, diffusion, and feedback mechanisms, demonstrating qualitative agreement with theoretical predictions and recent ecological findings.

However, the current implementation faces practical limitations. Simulations were primarily conducted on a 101×101 grid due to computational constraints. In contrast, typical ecological studies often require domain sizes of 256×256 or larger to fully capture pattern wavelength selection and long-range interactions. The fine spatial and temporal resolutions needed for accurate vegetation pattern simulation significantly increase the computational load, leading to long simulation runtimes.

Despite these limitations, this project demonstrates that discrete-event simulation frameworks like Cell-DEVS can effectively model complex spatiotemporal phenomena in ecology. The results validate the potential of using event-driven, modular approaches for scalable environmental simulations and lay the groundwork for further extensions toward larger, more realistic domains.

A. Future Work

Future efforts will focus on several key areas:

- **GPU Acceleration:** Implementing parallelized versions of Cell-DEVS using OpenCL or CUDA to dramatically reduce computation time and enable the simulation of larger domains (e.g., 256×256 grids and beyond).
- **Extended Ecological Models:** Incorporating additional ecological factors such as nutrient cycling, multi-species interactions, or topographical variations to create more comprehensive vegetation models.
- **Integration with Empirical Data:** Coupling simulation outputs with satellite imagery or field measurements to calibrate model parameters and validate emergent patterns against real-world observations.
- **Adaptive Resolution Methods:** Exploring techniques such as adaptive mesh refinement to focus computational resources on active regions of the domain, improving efficiency while maintaining accuracy.
- **Hybrid DEVS–Machine Learning Approaches:** Investigating how data-driven methods, such as neural networks, could assist in accelerating pattern prediction, parameter tuning, or uncertainty quantification within the Cell-DEVS framework.

Through these extensions, the project aims to transform the current prototype into a powerful, scalable platform for studying complex vegetation dynamics, ecological resilience, and environmental pattern formation in greater detail.

Acknowledgment

The author acknowledges the use of AI-based writing assistance (e.g., ChatGPT) for grammar checking, text organization, and formatting support during the preparation of this report. All simulation designs, model implementations, and results analysis were independently conducted by the author.

References

[1] A. M. Turing, "The chemical basis of morphogenesis," *Philosophical Transactions of the Royal Society of London. Series B, Biological Sciences*, vol. 237, no. 641, pp. 37–72, Aug. 1952, doi:10.1098/rstb.1952.0012.

[2] P. Gray and S. K. Scott, "Autocatalytic reactions in the isothermal, continuous stirred tank reactor: Oscillations and instabilities in the system $A + 2B \rightarrow 3B; B \rightarrow C$," *Chemical Engineering Science*, vol. 39, no. 6, pp. 1087–1097, 1984, doi:10.1016/0009-2509(84)87017-7.

[3] C. A. Klausmeier, "Regular and irregular patterns in semiarid vegetation," *Science*, vol. 284, no. 5421, pp. 1826–1828, Jun. 1999, doi:10.1126/science.284.5421.1826.

[4] M. Rietkerk, M. C. Boerlijst, F. van Langevelde, R. HilleRisLambers, J. van de Koppel, L. Kumar, H. H. T. Prins, and A. M. de Roos, "Self-organization of vegetation in arid ecosystems," *The American Naturalist*, vol. 160, no. 4, pp. 524–530, 2002, doi:10.1086/342078.

[5] J. E. Pearson, "Complex patterns in a simple system," *Science*, vol. 261, no. 5118, pp. 189–192, Jul. 1993, doi:10.1126/science.261.5118.189.

[6] Biological Modeling Project, "Gray-Scott Model Overview," Available: https://biologicalmodeling.org/prologue/gray-scott

[7] J. von Hardenberg, E. Meron, M. Shachak, and Y. Zarmi, "Diversity of vegetation patterns and desertification," *Physical Review Letters*, vol. 87, no. 19, Art. no. 198101, Oct. 2001, doi:10.1103/PhysRevLett.87.198101.

[8] Z. Ge, "The hidden order of Turing patterns in arid and semi-arid vegetation ecosystems," *Proceedings of the National Academy of Sciences*, vol. 120, no. 42, Art. no. e2306514120, Oct. 2023, doi:10.1073/pnas.2306514120.

[9] S. Kondo and R. Asai, "A reaction-diffusion wave on the skin of the marine angelfish *Pomacanthus*," *Nature*, vol. 376, pp. 765–768, Aug. 1995, doi:10.1038/376765a0.

[10] V. Volpert and S. Petrovskii, "Reaction-diffusion waves in biology: new trends, recent developments," *Phys. Life Rev.*, vol. 52, pp. 1–20, 2025, doi:10.1016/j.plrev.2024.11.007.